

Large deviations of current for the symmetric simple exclusion process on a semi-infinite line and on an infinite line with slow bonds

Kapil Sharma,^{1,*} Soumyabrata Saha,^{1,†} Sandeep Jangid,^{1,‡} and Tridib Sadhu^{1,§}

¹*Department of Theoretical Physics, Tata Institute of Fundamental Research, Homi Bhabha Road, Mumbai 400005, India*

(Dated: May 2, 2024)

Two of the most influential exact results for classical one-dimensional diffusive transport are the exact results of current statistics for the symmetric simple exclusion process in the stationary state on a finite line coupled with two unequal reservoirs at the boundary and in the non-stationary state on an infinite line. We present the corresponding result for the intermediate geometry of a semi-infinite line coupled with a single reservoir. These results are obtained using the fluctuating hydrodynamics framework of the macroscopic fluctuation theory and confirmed by rare event simulations using a cloning algorithm. Our exact result enables us to address the corresponding problem on an infinite line in the presence of a slow region and several related problems.

Current fluctuations in non-equilibrium transport have long been a subject of interest in both classical and quantum contexts [1–4]. The major interest in these investigations lies in the full counting statistics in terms of large deviations of current fluctuations. Apart from being a contender for extension of free energy for out-of-equilibrium systems, large deviation function (ldf) in general can characterize various peculiarities of non-equilibrium conditions, such as non-local response, emergent symmetries, and low-dimensional phase transitions [2, 5]. However, estimating ldf poses a major challenge, often requiring specialized integrability techniques [6–8] tailored to curated models or clever numerical sampling schemes of rare-probability events [9, 10]. Exact results play an important role in the landscape of non-equilibrium physics, providing a benchmark for affirming qualitative predictions of approximate methods. Our work in this *Letter* presents a non-trivial addition to this list of exact results.

Among the simplest and most widely studied models of classical transport is the symmetric simple exclusion process (SSEP) [11–13], a classical interacting many-particle stochastic dynamics on a lattice. The SSEP, along with its driven variants, has attained the status of a paradigmatic model in non-equilibrium statistical physics [7, 14]. Two celebrated exact results for the SSEP concern the large deviations of current on a finite lattice coupled with two unequal reservoirs and on an infinite lattice starting with a non-stationary state. The large deviations for these geometries are obtained using the additivity conjecture [15, 16] and integrability methods, such as the diagonalization of tilted matrix [17] or the matrix product states [6, 18] for the finite lattice, and the Bethe ansatz [19] for the infinite lattice. These microscopic results were subsequently verified [20–22] using a fluctuating hydrodynamics approach [23, 24], now famously known as the Macroscopic Fluctuation Theory (MFT). The two geometries represent distinct non-equilibrium scenarios: a stationary state for finite systems and a time-dependent state relaxing towards an asymptotic equilib-

rium state for infinite systems. They illuminate crucial differences in their fluctuations. The finite system, in the long run, holds no memory of the initial state, while the infinite system exhibits an unusual dependence on the initial state even at large times [25, 26].

In this *Letter*, we consider an intermediate scenario of the SSEP on a semi-infinite lattice [27, 28] coupled to a reservoir at one end with a density that is different from the initial average density of the system. This elucidates a non-stationary out-of-equilibrium regime evolving into an asymptotic state in equilibrium with the reservoir, although the dynamical quantities remain sensitive to the initial conditions [29]. Only limited results are known for this intermediate geometry [29–31], particularly because extending the aforementioned integrability methods for this geometry proves challenging. Even the solution via the MFT poses a considerable challenge. We tackled these difficulties within the MFT and obtained an exact result for the ldf of current on the semi-infinite geometry, which is our main result. Additionally, this exact result further enables us to obtain the ldf of current in the presence of a slow region, both in the semi-infinite and infinite geometry.

The MFT emerged in the early 2000s from the seminal works of Bertini, De Sole, Gabrielli, Jona-Lasinio, and Landim [23, 32], which presented a general framework for characterising non-equilibrium fluctuations of diffusive systems. This powerful framework has successfully led to exact results of large deviations in exclusion processes [20–23, 33] and related transport models [23, 34–37].

For the semi-infinite line, we solved the large deviations of current by uncovering a symmetry in the corresponding infinite line problem and subsequently mapping it to the former geometry. The symmetry and the mapping are possible due to the specific nature of the Euler-Lagrange equations and boundary conditions of the associated variational problem within MFT. These techniques, however, could not be obviously exploited within microscopic approaches. Our exact result is a testament

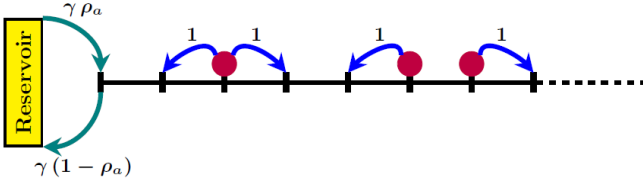


FIG. 1. SSEP on a semi-infinite lattice coupled with the boundary reservoir of density ρ_a , where γ represents the coupling strength with the reservoir.

to the power of the MFT for non-equilibrium systems that are formidable to approach by microscopic analysis.

The model and the main results: The SSEP describes a system of continuous-time random walkers on a lattice subject to a hard-core repulsion, preventing more than one particle from occupying a site at any given time. Due to this exclusion, each site i is described by an occupation number $n_i(\tau)$ at time τ , which takes binary values of 1 and 0 depending on whether the site is occupied or empty, respectively. The dynamics are stochastic, allowing each particle to hop to an adjacent site with a unit rate only if the target site is empty. We consider a semi-infinite \mathbb{Z}^+ lattice coupled to a boundary reservoir of density ρ_a , modelled by the jump rates in Fig. 1. Initially, particles are distributed following a Bernoulli distribution with a uniform average density ρ_b .

Our results are for the time-integrated current, Q_T , which represents the total flux of particles from the reservoir into the system over a period T . In the hydrodynamic description [38], expressed in terms of coarse-grained density $\rho(\frac{i}{\sqrt{T}}, \frac{\tau}{T}) \simeq n_i(\tau)$, the flux

$$Q_T = \sqrt{T} \int_0^\infty dx [\rho(x, 1) - \rho(x, 0)] \quad (1)$$

measures the net change in the number of particles in the system. In the large time T limit, its generating function has the asymptotics

$$\langle e^{\lambda Q_T} \rangle \sim e^{\sqrt{T} \mu_{\text{si}}(\lambda, \rho_a, \rho_b)}. \quad (2a)$$

Here, the scaled cumulant generating function (scgf) $\mu_{\text{si}}(\lambda, \rho_a, \rho_b)$ (subscript ‘si’ denotes semi-infinite) is given by

$$\mu_{\text{si}}(\lambda, \rho_a, \rho_b) = \int_{-\infty}^\infty \frac{dk}{2\pi} \log [1 + 4\omega(1 + \omega) e^{-k^2}] \quad (2b)$$

where ω is a function of the parameters defined as: [19, 26]

$$\omega(\lambda, \rho_a, \rho_b) = \rho_a(1 - \rho_b)(e^\lambda - 1) + \rho_b(1 - \rho_a)(e^{-\lambda} - 1) \quad (2c)$$

This dependence of scgf on λ, ρ_a , and ρ_b through a single function ω arises from a symmetry of the underlying dynamics of the SSEP [17, 19, 39]. It is instructive to compare (2b) with the corresponding result for the infinite line [19].

The scgf (2b) encapsulates all cumulants of Q_T in the long-time limit. While the first three cumulants were initially reported in [29], we present here the fourth cumulant for $\rho_a = \rho_b = \rho$:

$$\langle Q_T^4 \rangle_c \simeq \frac{4}{\sqrt{\pi}} \rho(1 - \rho) [1 - 12(\sqrt{2} - 1)\rho(1 - \rho)]. \quad (3)$$

The expression (2b) is consistent with the known [29] result in the low-density limit. Similar to the infinite line case [25], the scgf (2b) also admits the Gallavotti-Cohen-type fluctuation symmetry:

$$\mu_{\text{si}}(\lambda, \rho_a, \rho_b) = \mu_{\text{si}}\left(\log \frac{\rho_b(1 - \rho_a)}{\rho_a(1 - \rho_b)} - \lambda, \rho_a, \rho_b\right). \quad (4)$$

Remarkably, the expression (2b) admits a Fredholm determinant representation:

$$\mu_{\text{si}}(\lambda, \rho_a, \rho_b) = \frac{1}{2\pi} \log \det [1 + K(x, y)] \quad (5)$$

with the kernel $K(x, y) = 4\omega(1 + \omega)\delta(x - y)\exp(\partial_x^2)$. Analogous Fredholm determinant structure is observed in related contexts for the position and current distribution of particles in TASEP [40] and the ASEP [41, 42]. This representation underscores a connection between TASEP and random matrix theory, as emphasized by Johansson [40]. However, a similar relationship for the SSEP is not apparent. Interestingly, an alternative representation of (2b) following [19]

$$\mu_{\text{si}}(\lambda, \rho_a, \rho_b) = \frac{1}{2\sqrt{\pi}} \sum_{n=1}^{\infty} \frac{(-1)^{n+1}}{n^{3/2}} [4\omega(1 + \omega)]^n \quad (6)$$

bears a striking resemblance to the scgf for the number of surviving particles in an assembly of annihilating random walkers (see eqn. (9.106) in [8]).

Numerical confirmation: For confirming our result (2b) based on the hydrodynamic description of SSEP, we have independently generated the scgf using numerical simulation based on a continuous time cloning algorithm [38, 43, 44] with 10^5 clones. The simulation result, plotted in Fig. 2, shows a good agreement with our theoretical result (6) for a reasonably large value of λ . Notable deviations at large λ are a consequence of finite-size effects [38], and improvement requires advanced computational resources, which are not currently available to us.

LDF: The scaling in (2a) corresponds to a large deviation asymptotics of the probability

$$\Pr(Q_T = q\sqrt{T}) \simeq e^{-\sqrt{T}\phi(q)} \quad (7)$$

where $\phi(q)$ is the large deviation function, related to $\mu(\lambda)$ (reference to $\rho_{a(b)}$ is ignored) by a Legendre-Fenchel transformation [45] $\phi(q) = \max_\lambda \{q\lambda - \mu(\lambda)\}$.

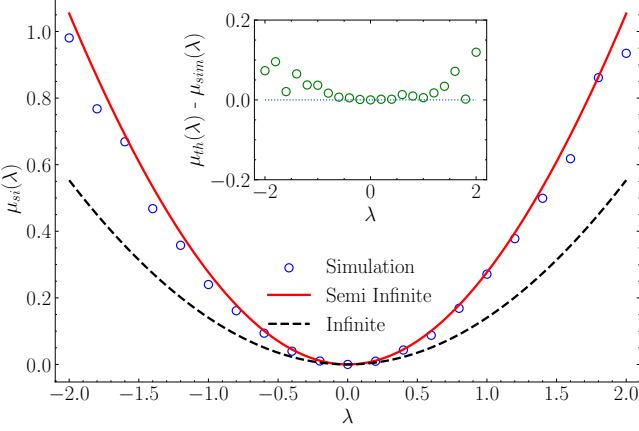


FIG. 2. The solid red line represents the theoretical result (2b) of the scgf for $\rho_a = \rho_b = 0.5$, while the corresponding numerical simulation result, obtained by the cloning algorithm, is indicated by circles. The results closely match in the range from $\lambda = -1.5$ to $\lambda = 1.5$. Beyond this range, finite-size effects [38] cause a noticeable deviations, as shown in the inset. For comparison, the corresponding scgf [19] for the infinite geometry is shown using the black dashed line.

Using the transformation, it is immediate that (4) reflects the symmetry:

$$\phi(q) - \phi(-q) = q \log \frac{\rho_b (1 - \rho_a)}{\rho_a (1 - \rho_b)} \quad (8)$$

Similarly, the asymptotics

$$\mu_{si}(\lambda, \rho_a, \rho_b) \simeq \frac{4\sqrt{2}}{3\pi} (\log \omega)^{3/2} \quad (9)$$

of (2b) for large positive λ correspond to the asymptotics of the ldf:

$$\phi(q) \simeq \frac{\pi^2 q^3}{24} - q \log (\rho_a (1 - \rho_b)) \quad (10)$$

for large positive q . A similar analysis for large negative q gives an asymptotics (10) with $q \rightarrow -q$ and $\rho_a \leftrightarrow \rho_b$.

The symmetry relation (8) and the asymptotics (10) are confirmed in the plot of the ldf in Fig. 3, generated by numerically evaluating the Legendre-Fenchel transformation of the scgf (2b). For the non-equilibrium condition $\rho_a \neq \rho_b$, the ldf is skewed.

Derivation: In the following, we outline our derivation of (2b) within the fluctuating hydrodynamic framework of MFT. The crucial idea behind MFT is to recognise the relevant hydrodynamic modes for a coarse-grained description of the dynamics and characterise the probability of their evolution in terms of an Action, which is analogous to the Martin-Siggia-Rose-Janssen-De Dominicis (MSRJD) Action [46–49] of the associated fluctuating hydrodynamics equation. For SSEP, the relevant hydrodynamic mode is the locally conserved density

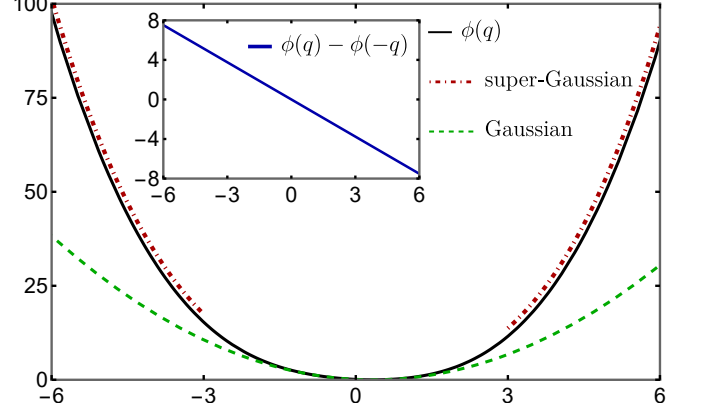


FIG. 3. The ldf, $\phi(q)$ indicated in solid line, with asymptotes (10) for large q indicated in red dashed lines. The green dashed line denotes the Gaussian ldf with the appropriate variance obtained from $\langle Q_T^2 \rangle$. The plots are for $\rho_a = 0.6$ and $\rho_b = 0.3$. The inset confirms the symmetry (8).

$\rho(x, t)$ evolving by [38]

$$\partial_t \rho = \partial_x^2 \rho + \frac{1}{T^{1/4}} \partial_x (\sigma(\rho) \eta) \quad (11)$$

where $\sigma(\rho) = 2\rho(1 - \rho)$ and $\eta(x, t)$ is a delta-correlated Gaussian white noise. Corresponding MSRJD-Action on the semi-infinite geometry is [38]:

$$S_0 = \mathcal{F} + \int_0^1 dt \int_0^\infty dx \left[\hat{\rho} \partial_t \rho - \frac{\sigma(\rho) (\partial_x \hat{\rho})^2}{2} + \partial_x \rho \partial_x \hat{\rho} \right] \quad (12)$$

where $\hat{\rho}$ is the response field and \mathcal{F} incorporates contributions from fluctuations in the initial state [25]. Within this description, the generating function $\langle e^{\lambda Q_T} \rangle = \int \mathcal{D}[\rho, \hat{\rho}] e^{-\sqrt{T} S_\lambda}$ with $S_\lambda = S_0 - \lambda Q_T / \sqrt{T}$ and Q_T in (1).

For large T , the path-integral is dominated by a saddle point, leading to:

$$\mu_{si}(\lambda) \simeq - \min_{\rho, \hat{\rho}} S_\lambda[\rho, \hat{\rho}] \equiv -S_\lambda[q_{si}, p_{si}] \quad (13)$$

where (q_{si}, p_{si}) is the least-Action path for $(\rho, \hat{\rho})$. This way, the problem reduces to solving the corresponding Euler-Lagrange equations:

$$\partial_t q_{si} = \partial_x [\partial_x q_{si} - \sigma(q_{si}) \partial_x p_{si}] \quad (14a)$$

$$\partial_t p_{si} = -\partial_x^2 p_{si} - \frac{\sigma'(q_{si})}{2} (\partial_x p_{si})^2 \quad (14b)$$

in the semi-infinite domain $x > 0$, with the temporal boundary conditions

$$p_{si}(x, 0) = \lambda + \int_{\rho_b}^{q(x, 0)} dr \frac{2}{\sigma(r)} \quad \text{and} \quad p_{si}(x, 1) = \lambda \quad (15)$$

where the integral in $p_{\text{si}}(x, 0)$ is the contribution from \mathcal{F} [25] for the initial state of the SSEP with Bernoulli measure. Additional spatial boundary conditions:

$$q_{\text{si}}(0, t) = \rho_a \quad \text{and} \quad p_{\text{si}}(0, t) = 0 \quad (16)$$

are due to the “fast-coupling” [33, 38] with reservoir.

This variational problem is reminiscent of the corresponding problem on the infinite line [25] with a Bernoulli-measured initial state with an average density ρ_a for $x < 0$ and ρ_b for $x > 0$. The only differences between the two problems are the domain x and the boundary conditions. The infinite line problem was formulated in [25] within MFT, which was recently solved in [22] by identifying an ingenious mapping to the classical integrable system and employing the inverse scattering method. Despite having small differences, the semi-infinite case poses a new nontrivial problem [50], which is incredibly difficult to solve.

A remarkable simplification arises for the special choice of initial density pair $(\rho_a, \rho_b) \equiv (\frac{1}{2}, 0)$ for the semi-infinite problem. For this choice of densities, there are no fluctuations in the initial state, which amounts to setting $\mathcal{F} = 0$ in (12) with the condition

$$q_{\text{si}}(x, 0) = 0. \quad (17)$$

The Euler-Lagrange equation for the corresponding variational problem (13) remains the same as in (14). The only difference comes in the initial condition in (15), which is now replaced by (17). This initial condition corresponds to the quenched averaging [25].

We now show that this quenched semi-infinite line problem has a direct mapping to the quenched infinite line problem with $(\rho_a, \rho_b) \equiv (1, 0)$ and fugacity $\tilde{\lambda} = 2\lambda$. For the latter problem, the Euler-Lagrange equation is the same [25] as in (14), but now on the entire real line x with the temporal boundary conditions

$$q_{\text{inf}}(x, 0) = \theta(-x) \quad \text{and} \quad p_{\text{inf}}(x, 1) = \tilde{\lambda} \theta(x) \quad (18)$$

(subscript ‘inf’ denotes infinite). It is trivial to check that the solution admits the symmetry

$$q_{\text{inf}}(x, t) = 1 - q_{\text{inf}}(-x, t) \quad (19)$$

$$p_{\text{inf}}(x, t) = \tilde{\lambda} - p_{\text{inf}}(-x, t) \quad (20)$$

which fixes the value of the fields at the origin

$$q_{\text{inf}}(0, t) = \frac{1}{2} \quad \text{and} \quad p_{\text{inf}}(0, t) = \frac{\tilde{\lambda}}{2} \quad (21)$$

at any time $0 < t < T$. This conclusion is an essential part of our observation, as now, the solution $q_{\text{inf}}(x, t)$ satisfies the boundary conditions (16, 17) of the semi-infinite problem. For a similar correspondence of the response field, we define

$$\tilde{p}(x, t) = p_{\text{inf}}(x, t) - \frac{\tilde{\lambda}}{2} \quad (22)$$

which too now replicate the boundary conditions $\tilde{p}(x, 1) = \lambda$ and $\tilde{p}(0, t) = 0$ of the semi-infinite line problem with $\tilde{\lambda} = 2\lambda$. The fields $(q_{\text{inf}}, \tilde{p})$ also satisfy the same Euler-Lagrange equations (14).

Consequently, the least-Action path $(q_{\text{si}}, p_{\text{si}})$ for the semi-infinite problem with $(\rho_a, \rho_b) \equiv (\frac{1}{2}, 0)$ and fugacity λ is related to the corresponding path $(q_{\text{inf}}, p_{\text{inf}})$ for the infinite problem with $(\rho_a, \rho_b) \equiv (1, 0)$ and fugacity 2λ by

$$q_{\text{si}}(x, t) = q_{\text{inf}}(x, t) \quad \text{and} \quad p_{\text{si}}(x, t) = p_{\text{inf}}(x, t) - \lambda \quad (23)$$

for $x \geq 0$. This correspondence relates the minimal Action of the two problems [38] resulting in our crucial observation

$$\mu_{\text{si}}\left(\lambda, \frac{1}{2}, 0\right) = \frac{1}{2} \mu_{\text{inf}}(2\lambda, 1, 0) \quad (24)$$

where the pre-factor $1/2$ comes from the half-domain of integration of x in (12). The latter scgf is known from the seminal work [19] of Derrida and Gerschenfeld which culminates in

$$\mu_{\text{si}}\left(\lambda, \frac{1}{2}, 0\right) = \frac{1}{2\pi} \int_{-\infty}^{\infty} dk \log [1 + (e^{2\lambda} - 1)e^{-k^2}]. \quad (25)$$

The result (25) is for the specific initial density pair $(\rho_a, \rho_b) \equiv (\frac{1}{2}, 0)$. For extending the results for other densities, we invoke a well-known rotational symmetry [25, 38, 39] of the minimal Action (13). Essentially, the least-Action paths for two sets of parameters $(\lambda, \rho_a, \rho_b)$ and $(\lambda', \rho_a', \rho_b')$ are related under a canonical transformation [25, 38, 39]. The symmetry results [19, 38, 39] in a dependence of the scgf on $(\lambda, \rho_a, \rho_b)$ through a single parameter

$$\mu_{\text{si}}(\lambda, \rho_a, \rho_b) = R_{\text{si}}(\omega(\lambda, \rho_a, \rho_b)) \quad (26)$$

where ω is defined in (2c). This invariance enables us to deduce [38] the function $R_{\text{si}}(\omega)$ from the result (25), leading to the expression (2b).

Slow coupling: Recent interests [29, 33, 51–55] in studying the effect of the coupling strength on the fluctuations can also be addressed in the semi-infinite problem. The result (2b) is independent of the coupling strength γ (see Fig. 1) as long as it is larger than $\mathcal{O}(T^{-1/2})$ [29]. For $\gamma = \Gamma/\sqrt{T}$, where Γ is a non-negative real-valued constant, the boundary-fluctuations are significant. For this slow coupling regime, a suitable extension [38] of the MFT formalism gives the modified scgf

$$\mu_{\text{si}}^{(\text{slow})}(\lambda, \rho_a, \rho_b) = \min_z \left[\Gamma \sinh^2(z \pm u) + R_{\text{si}}(\sinh^2 z) \right] \quad (27)$$

with $\sinh^2 u = \omega(\lambda, \rho_a, \rho_b)$. The result can be alternatively obtained following the additivity argument [56], where contributions in (27) are separately from the single bond joining the bath and the system, and the system itself, optimised over the density at their common site. In the $\Gamma \rightarrow \infty$ limit, (2b) is recovered from (27).

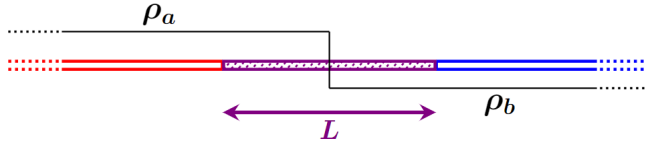


FIG. 4. An infinite SSEP with slow regions of length L , initialized with an average step density profile.

Slow region on infinite line: The result (26) aids in addressing another significant problem about current fluctuations on an infinite line with a finite slow region around the origin, where the current is measured (see illustration in Fig. 4). Similar to (27), the scgf can be derived [56] by combining the contributions from two semi-infinite lines joined via a finite region of length $L \ll \sqrt{T}$ with slow jump rates $\gamma = \Gamma/\sqrt{T}$. This yields

$$\mu_{\text{inf}}^{(\text{slow})}(\lambda, \rho_a, \rho_b) = \min_{z_a, z_b} \left[R_{\text{si}}(\sinh^2 z_a) + \frac{\Gamma}{L} (z_a + z_b - u)^2 + R_{\text{si}}(\sinh^2 z_b) \right] \quad (28)$$

with $\sinh^2 u = \omega(\lambda, \rho_a, \rho_b)$. For the middle term on the right-hand side of (28), we used the known result [17] of the scgf for a finite SSEP. In the $\Gamma \rightarrow \infty$ limit, (2b) is recovered [38] from (28).

Conclusions: Based on our exact results, several interesting conclusions can be drawn. A symmetry of the MFT-Action [25] extends results for models with a quadratic mobility $\sigma(q) = 2Aq(B - q)$, where A and B are arbitrary constants, culminating in $\mu_\sigma(\lambda, \rho_a, \rho_b) = \frac{1}{A} \mu_{\text{ssep}}(\omega(AB\lambda, \frac{\rho_a}{B}, \frac{\rho_b}{B}))$.

The semi-infinite line result provides immediate solutions for two problems. The first problem [57] concerns an infinite line SSEP with fast injection at a single site, a scenario which gained prominence in recent years [58–60]. At long times t , the net injection of particles N_t on an empty lattice follows the asymptotics $\langle e^{\lambda N_t} \rangle \sim e^{\sqrt{t} 2 \mu_{\text{si}}(\lambda, 1, 0)}$ with μ_{si} in (2b). The second problem concerns the survival probability $P_t(k)$ of the k^{th} particle up to time t in a *fully* packed SSEP on \mathbb{Z}^+ in the presence of an absorbing site at the origin. The large deviations asymptotics (7) and the relation $P_t(k) = P(Q_t > k)$, where $P(Q_t > k)$ is the cumulative probability of integrated current, result in a stretched exponential decay $P_t(k) \sim e^{-\sqrt{t/\tau_s}}$ for $k < 2\sqrt{t/\pi}$ at long times t , with $\tau_s = [\phi(-k/\sqrt{t})]^{-2}$.

Similar stretched exponential decays are noted in kinetically constrained models [61–64]. A well-known example is energy-conserving spin-flip dynamics, where spin auto-correlation is predicted to decay as $e^{-\sqrt{t/\tau}}$, with τ remaining undetermined [62]. It is realized [64] that the domain-wall dynamics is equivalent to the infinite line SSEP at a uniform density ρ , equal to domain-wall-density. This equivalence straightforwardly gives

$\tau = [\mu(i\pi, \rho, \rho)]^{-2}$, where $\mu(\lambda, \rho_a, \rho_b)$ is the scgf of the infinite line problem [19]. A similar result holds in the presence of slow regions in the domain wall dynamics, relating to the corresponding result (28).

There remain several related open problems of immediate interest. Most prominent among them is the scgf for fixed (quenched) initial states at arbitrary densities, which remains intractable for all geometries of SSEP. The only available non-trivial result [25] is for the infinite line SSEP at a uniform density $\rho = 1/2$, obtained by establishing a relation with the fluctuating (annealed) initial state. A similar mapping for the semi-infinite geometry yields the quenched scgf

$$\mu_{\text{que}}\left(\lambda, \frac{1}{2}, \frac{1}{2}\right) = \int_{-\infty}^{\infty} \frac{dk}{\pi\sqrt{8}} \log [1 + \sinh^2(\lambda) e^{-k^2}] \quad (29)$$

Another pressing open question is the least-Action path at arbitrary densities for the semi-infinite line. In general directions, an extension of the problem in higher dimensions would be interesting, where only limited results are available [65]. From a practical point of view, the emergence of the infinite line SSEP in quantum circuits [4] is exciting, and a semi-infinite analog of the problem would be worth exploring. Along similar lines, extensions of our results for quantum analogues of the SSEP [66] or for integrable models using generalized hydrodynamics [67] would be timely.

We acknowledge the financial support of the Department of Atomic Energy, Government of India, under Project Identification No. RTI 4002. TS thanks Mustansir Barma for introducing him to the works on stretched exponential decays.

* kapil.sharma@tifr.res.in

† soumyabrata.saha@tifr.res.in

‡ sandeep.jangid@tifr.res.in

§ tridib@theory.tifr.res.in

- [1] H. Lee, L. S. Levitov, and A. Y. Yakovets, Universal statistics of transport in disordered conductors, *Phys. Rev. B* **51**, 4079 (1995).
- [2] B. Derrida, Non-equilibrium steady states: Fluctuations and large deviations of the density and of the current, *J. Stat. Mech.* **2007**, P07023 (2007).
- [3] T. Banerjee, S. N. Majumdar, A. Rosso, and G. Schehr, Current fluctuations in noninteracting run-and-tumble particles in one dimension, *Phys. Rev. E* **101**, 052101 (2020).
- [4] E. McCulloch, J. De Nardis, S. Gopalakrishnan, and R. Vasseur, Full counting statistics of charge in chaotic many-body quantum systems, *Phys. Rev. Lett.* **131**, 210402 (2023).
- [5] G. Jona-Lasinio, From fluctuations in hydrodynamics to nonequilibrium thermodynamics, *Prog. Theor. Phys. Suppl.* **184**, 262–275 (2010).
- [6] A. Lazarescu, The physicist's companion to current fluc-

tuations: One-dimensional bulk-driven lattice gases, *J. Phys. A: Math. Theor.* **48**, 503001 (2015).

[7] K. Mallick, The exclusion process: A paradigm for non-equilibrium behaviour, *Physica A* **418**, 17–48 (2015).

[8] G. M. Schütz, Exactly solvable models for many-body systems far from equilibrium, in *Phase Transitions and Critical Phenomena*, Vol. 19, edited by C. Domb and J. L. Lebowitz (Academic Press, 2001) p. 1–251.

[9] C. Pérez-Espigares and P. I. Hurtado, Sampling rare events across dynamical phase transitions, *Chaos* **29**, 083106 (2019).

[10] A. K. Hartmann, *Big Practical Guide to Computer Simulations*, 2nd ed. (World Scientific, 2015).

[11] H. Spohn, *Large Scale Dynamics of Interacting Particles* (Springer Berlin, Heidelberg, 1991).

[12] C. Kipnis and C. Landim, *Scaling Limits of Interacting Particle Systems* (Springer Berlin, Heidelberg, 1999).

[13] T. M. Liggett, *Stochastic Interacting Systems: Contact, Voter and Exclusion Processes* (Springer Berlin, Heidelberg, 1999).

[14] T. Chou, K. Mallick, and R. K. P. Zia, Non-equilibrium statistical mechanics: from a paradigmatic model to biological transport, *Rep. Prog. Phys.* **74**, 116601 (2011).

[15] T. Bodineau and B. Derrida, Current fluctuations in nonequilibrium diffusive systems: An additivity principle, *Phys. Rev. Lett.* **92**, 180601 (2004).

[16] T. Bodineau and B. Derrida, Cumulants and large deviations of the current through non-equilibrium steady states, *C. R. Physique* **8**, 540–555 (2007).

[17] B. Derrida, B. Douçot, and P. E. Roche, Current fluctuations in the one-dimensional symmetric exclusion process with open boundaries, *J. Stat. Phys.* **115**, 717–748 (2004).

[18] M. Gorissen, A. Lazarescu, K. Mallick, and C. Vanderzande, Exact current statistics of the asymmetric simple exclusion process with open boundaries, *Phys. Rev. Lett.* **109**, 170601 (2012).

[19] B. Derrida and A. Gerschenfeld, Current fluctuations of the one dimensional symmetric simple exclusion process with step initial condition, *J. Stat. Phys.* **136**, 1–15 (2009).

[20] L. Bertini, A. De Sole, D. Gabrielli, G. Jona-Lasinio, and C. Landim, Current fluctuations in stochastic lattice gases, *Phys. Rev. Lett.* **94**, 030601 (2005).

[21] L. Bertini, A. De Sole, D. Gabrielli, G. Jona-Lasinio, and C. Landim, Non equilibrium current fluctuations in stochastic lattice gases, *J. Stat. Phys.* **123**, 237–276 (2006).

[22] K. Mallick, H. Moriya, and T. Sasamoto, Exact solution of the macroscopic fluctuation theory for the symmetric exclusion process, *Phys. Rev. Lett.* **129**, 040601 (2022).

[23] L. Bertini, A. De Sole, D. Gabrielli, G. Jona-Lasinio, and C. Landim, Macroscopic fluctuation theory, *Rev. Mod. Phys.* **87**, 593 (2015).

[24] G. Jona-Lasinio, Review article: Large fluctuations in non-equilibrium physics, *Nonlin. Processes Geophys.* **30**, 253–262 (2023).

[25] B. Derrida and A. Gerschenfeld, Current fluctuations in one dimensional diffusive systems with a step initial density profile, *J. Stat. Phys.* **137**, 978–1000 (2009).

[26] P. L. Krapivsky and B. Meerson, Fluctuations of current in nonstationary diffusive lattice gases, *Phys. Rev. E* **86**, 031106 (2012).

[27] T. M. Liggett, Ergodic theorems for the asymmetric simple exclusion process, *Trans. Am. Math. Soc.* **213**, 237 (1975).

[28] S. Grosskinsky, *Phase transitions in nonequilibrium stochastic particle systems with local conservation laws*, Ph.D. thesis, Technical University of Munich (2004).

[29] S. Saha and T. Sadhu, Current fluctuations in a semi-infinite line, *J. Stat. Mech.* **2023**, 073207 (2023).

[30] L. Williams and T. Sasamoto, Combinatorics of the asymmetric exclusion process on a semi-infinite lattice (2012), arXiv:1204.1114 [cond-mat.stat-mech].

[31] H. G. Duhart, P. Mörters, and J. Zimmer, The semi-infinite asymmetric exclusion process: Large deviations via matrix products, *Potential Anal.* **48**, 301–323 (2018).

[32] L. Bertini, A. De Sole, D. Gabrielli, G. Jona-Lasinio, and C. Landim, Fluctuations in stationary nonequilibrium states of irreversible processes, *Phys. Rev. Lett.* **87**, 040601 (2001).

[33] S. Saha and T. Sadhu, Large deviations in the symmetric simple exclusion process with slow boundaries: A hydrodynamic perspective (2023), arXiv:2310.11350v2 [cond-mat.stat-mech].

[34] A. Krajenbrink and P. Le Doussal, Inverse scattering of the Zakharov-Shabat system solves the weak noise theory of the Kardar-Parisi-Zhang equation, *Phys. Rev. Lett.* **127**, 064101 (2021).

[35] E. Bettelheim, N. R. Smith, and B. Meerson, Inverse scattering method solves the problem of full statistics of nonstationary heat transfer in the Kipnis-Marchioro-Presutti model, *Phys. Rev. Lett.* **128**, 130602 (2022).

[36] T. Agranov, S. Ro, Y. Kafri, and V. Lecomte, Macroscopic fluctuation theory and current fluctuations in active lattice gases, *SciPost Phys.* **14**, 045 (2023).

[37] E. Bettelheim and B. Meerson, Complete integrability of the problem of full statistics of nonstationary mass transfer in the simple inclusion process (2024), arXiv:2403.19536v2 [cond-mat.stat-mech].

[38] See Supplementary Materials.

[39] V. Lecomte, A. Imparato, and F. van Wijland, Current fluctuations in systems with diffusive dynamics, in and out of equilibrium, *Prog. Theor. Phys. Suppl.* **184**, 276–289 (2010).

[40] K. Johansson, Shape fluctuations and random matrices, *Comm. Math. Phys.* **209**, 437–476 (2000).

[41] C. A. Tracy and H. Widom, A fredholm determinant representation in ASEP, *J. Stat. Phys.* **132**, 291–300 (2008).

[42] C. A. Tracy and H. Widom, Total current fluctuations in the asymmetric simple exclusion process, *J. Math. Phys.* **50**, 095204 (2009).

[43] C. Giardina, J. Kurchan, and L. Peliti, Direct evaluation of large-deviation functions, *Phys. Rev. Lett.* **96**, 120603 (2006).

[44] V. Lecomte and J. Tailleur, A numerical approach to large deviations in continuous time, *J. Stat. Mech.* **2007**, P03004 (2007).

[45] H. Touchette, The large deviation approach to statistical mechanics, *Phys. Rep.* **478**, 1–69 (2009).

[46] P. C. Martin, E. D. Siggia, and H. A. Rose, Statistical dynamics of classical systems, *Phys. Rev. A* **8**, 423 (1973).

[47] H. K. Janssen, On a lagrangean for classical field dynamics and renormalization group calculations of dynamical critical properties, *Z. Physik B* **23**, 377–380 (1976).

[48] C. De Dominicis, Dynamics as a substitute for replicas in systems with quenched random impurities, *Phys. Rev. B* **18**, 4913 (1978).

[49] C. De Dominicis and L. Peliti, Field-theory renormalization and critical dynamics above T_c : Helium, antiferromagnets, and liquid-gas systems, *Phys. Rev. B* **18**, 353 (1978).

[50] M. J. Ablowitz and H. Segur, The inverse scattering transform: Semi-infinite interval, *J. Math. Phys.* **16**, 1054–1056 (1975).

[51] R. Baldasso, O. Menezes, A. Neumann, and R. R. Souza, Exclusion process with slow boundary, *J. Stat. Phys.* **167**, 1112–1142 (2017).

[52] T. Franco, P. Gonçalves, and A. Neumann, Non-equilibrium and stationary fluctuations of a slowed boundary symmetric exclusion, *Stoch. Process. Their Appl.* **129**, 1413–1442 (2019).

[53] P. Gonçalves, M. Jara, O. Menezes, and A. Neumann, Non-equilibrium and stationary fluctuations for the SSEP with slow boundary, *Stoch. Process. Their Appl.* **130**, 4326–4357 (2020).

[54] C. Erignoux, P. Gonçalves, and G. Nahum, Hydrodynamics for SSEP with non-reversible slow boundary dynamics: Part I, the critical regime and beyond, *J. Stat. Phys.* **181**, 1433–1469 (2020).

[55] C. Erignoux, P. Gonçalves, and G. Nahum, Hydrodynamics for SSEP with non-reversible slow boundary dynamics: Part II, below the critical regime, *ALEA, Lat. Am. J. Probab. Math. Stat.* **17**, 791–823 (2020).

[56] B. Derrida, O. Hirschberg, and T. Sadhu, Large deviations in the symmetric simple exclusion process with slow boundaries, *J. Stat. Phys.* **182**, 15 (2021).

[57] P. L. Krapivsky, Symmetric exclusion process with a localized source, *Phys. Rev. E* **86**, 041103 (2012).

[58] P. L. Krapivsky and D. Stefanovic, Lattice gases with a point source, *J. Stat. Mech.* **2014**, P09003 (2014).

[59] P. L. Krapivsky, K. Mallick, and D. Sels, Free fermions with a localized source, *J. Stat. Mech.* **2019**, 113108 (2019).

[60] P. L. Krapivsky, K. Mallick, and D. Sels, Free bosons with a localized source, *J. Stat. Mech.* **2020**, 063101 (2020).

[61] J. L. Skinner, Kinetic Ising model for polymer dynamics: Applications to dielectric relaxation and dynamic depolarized light scattering, *J. Chem. Phys.* **79**, 1955–1964 (1983).

[62] H. Spohn, Stretched exponential decay in a kinetic Ising model with dynamical constraint, *Commun. Math. Phys.* **125**, 3–12 (1989).

[63] V. Gupta, S. K. Nandi, and M. Barma, Size-stretched exponential relaxation in a model with arrested states, *Phys. Rev. E* **102**, 022103 (2020).

[64] S. Mukherjee, P. Pareek, M. Barma, and S. K. Nandi, Stretched exponential to power-law: crossover of relaxation in a kinetically constrained model, *J. Stat. Mech.* **2024**, 023205 (2024).

[65] E. Akkermans, T. Bodineau, B. Derrida, and O. Shpielberg, Universal current fluctuations in the symmetric exclusion process and other diffusive systems, *EPL* **103**, 20001 (2013).

[66] D. Bernard and T. Jin, Open quantum symmetric simple exclusion process, *Phys. Rev. Lett.* **123**, 080601 (2019).

[67] B. Doyon, Lecture notes on generalised hydrodynamics, *SciPost Phys. Lect. Notes* , 18 (2020).

Supplementary Material: Large deviations of current for the symmetric simple exclusion process on a semi-infinite line

Kapil Sharma,^{1,*} Soumyabrata Saha,^{1,†} Sandeep Jangid,^{1,‡} and Tridib Sadhu^{1,§}

¹*Department of Theoretical Physics, Tata Institute of Fundamental Research, Homi Bhabha Road, Mumbai 400005, India*

(Dated: May 1, 2024)

We show that the MFT-Action for the semi-infinite line can be mapped onto the corresponding infinite line problem and that it admits a rotational symmetry. We discuss the numerical details and show the effects of system size, time of simulations and the number of clones in the numerical estimation of the scgf. Finally, we derive the scgf for the infinite line with a finite region of slow bonds and the fluctuating hydrodynamic equations for the infinite line with single slow bond.

CONTENTS

Action formulation for the semi-infinite SSEP	S-1
Relation between generating function of finite and semi-infinite line	S-2
Rotational Symmetry of MFT action: “ ω ” dependence	S-2
Numerical details: Cloning algorithm	S-3
Infinite SSEP with multiple slow bonds: current fluctuations	S-3
Infinite SSEP with a single slow bond: fluctuating hydrodynamics	S-7
Recovering the infinite line results	S-8
References	S-8

ACTION FORMULATION FOR THE SEMI-INFINITE SSEP

The moment-generating function is given as a path integral

$$\langle e^{\lambda Q_T} \rangle = \int [D\rho][D\hat{\rho}] e^{-\sqrt{T} S[\rho, \hat{\rho}]} \quad (\text{S-1})$$

where the action is

$$S[\rho, \hat{\rho}] = -\lambda \int_0^\infty dx [\rho(x, 1) - \rho(x, 0)] + \mathcal{F}[\rho(x, 0)] + \int_0^1 dt \left[\int_0^\infty dx [\hat{\rho}(x, t) \partial_t \rho(x, t)] - H[\rho, \hat{\rho}] \right] \quad (\text{S-2})$$

The term \mathcal{F} in the action measures the contribution due to a random initial configuration, which for the annealed ensemble is the free energy of the initial equilibrium state of uniform average density ρ_b . For the semi-infinite line, this is given by

$$\mathcal{F}[\rho(x, 0)] = \int_0^\infty dx \int_{\rho_b}^{\rho(x, 0)} dr \frac{2D(r)}{\sigma(r)} [\rho(x, 0) - r] \quad (\text{S-3})$$

For the SSEP, we set the diffusivity $D(\rho) = 1$ and the mobility $\sigma(\rho) = 2\rho(1 - \rho)$ in the above and the following expressions.

The effective Hamiltonian in the action formulation is

$$H[\rho, \hat{\rho}] = H_{\text{bdry}}[\rho(0, t), \hat{\rho}(0, t)] + \int_0^\infty dx \left[\frac{\sigma(\rho)}{2} \partial_x \hat{\rho}(x, t) - D(\rho) \partial_x \rho(x, t) \right] \partial_x \hat{\rho}(x, t) \quad (\text{S-4})$$

where H_{bdry} measures the contribution due to coupling with the reservoir at the left boundary. For the SSEP, the boundary part of the Hamiltonian is given by [1]

$$H_{\text{bdry}}[\rho_0, \hat{\rho}_0] = \gamma \sqrt{T} [(e^{\hat{\rho}_0} - 1) \rho_a (1 - \rho_0) + (e^{-\hat{\rho}_0} - 1) \rho_0 (1 - \rho_a)] \quad (\text{S-5})$$

We take $\gamma \sim T^{-\theta}$ where $\theta \in \mathbb{R}$ [2–4] such that $\theta < 1/2$ represents the fast coupling regime while $\theta > 1/2$ represents the slow coupling regime.

For the marginal coupling case ($\theta = 1/2$) which separates the two regimes, we take $\gamma = \Gamma/\sqrt{T}$ where $\Gamma \in \mathbb{R}_{\geq 0}$. In the limit $\Gamma \rightarrow \infty$, we recover the fast coupling results while in the limit $\Gamma \rightarrow 0$, we recover the slow coupling results [1, 4].

RELATION BETWEEN GENERATING FUNCTION OF FINITE AND SEMI-INFINITE LINE

For the infinite line starting with the density $(\rho_a, \rho_b) \equiv (1, 0)$, the quenched and annealed ensembles are equivalent and the scaled generating function will be given by the minimal action

$$\mu_{\text{inf}}(\tilde{\lambda}, 1, 0) = \tilde{\lambda} \int_0^\infty dx [q(x, 1) - q(x, 0)] - \int_0^1 dt \int_{-\infty}^\infty dx [p \partial_t q - q (1 - q) (\partial_x p)^2 + \partial_x q \partial_x p] \quad (\text{S-6})$$

and for the semi-infinite line with $(\rho_a, \rho_b) \equiv (\frac{1}{2}, 0)$

$$\mu_{\text{si}}\left(\lambda, \frac{1}{2}, 0\right) = \lambda \int_0^\infty dx [q(x, 1) - q(x, 0)] - \int_0^1 dt \int_0^\infty dx [p \partial_t q - q (1 - q) (\partial_x p)^2 + \partial_x q \partial_x p] \quad (\text{S-7})$$

Now, the symmetry relations in optimal profiles of the infinite line

$$q_{\text{inf}}(x, t) = 1 - q_{\text{inf}}(-x, t) \quad (\text{S-8})$$

$$p_{\text{inf}}(x, t) = \tilde{\lambda} - p_{\text{inf}}(-x, t) \quad (\text{S-9})$$

reduces the problem of x -integral over the entire line to that over the positive half-line only. Further, the mappings

$$p_{\text{si}}(x, t) = p_{\text{inf}}(x, t) - \frac{\tilde{\lambda}}{2} \quad (\text{S-10})$$

$$q_{\text{si}}(x, t) = q_{\text{inf}}(x, t) \quad (\text{S-11})$$

with $\tilde{\lambda} = 2\lambda$, leads to the relation

$$\mu_{\text{si}}\left(\lambda, \frac{1}{2}, 0\right) = \frac{1}{2} \mu_{\text{inf}}(2\lambda, 1, 0) \quad (\text{S-12})$$

from (S-6) and (S-7).

ROTATIONAL SYMMETRY OF MFT ACTION: “ ω ” DEPENDENCE

This discussion follows from the ref [5, 6]. From a direct correspondence to the Heisenberg spin chain model, there exists an underlying rotational symmetry for the action in the annealed case, that allows us to relate a set of optimal profiles (q, p) with the parameters $(\lambda, \rho_a, \rho_b)$ to another set of optimal profiles (q', p') with a different set of parameters $(\lambda, \rho'_a, \rho'_b)$ by a canonical transformation. This transformation relates two variational problems with the corresponding parameters $(\lambda, \rho_a, \rho_b)$ and $(\lambda', \rho'_a, \rho'_b)$ when $\omega(\lambda, \rho_a, \rho_b) = \omega'(\lambda', \rho'_a, \rho'_b)$. Now following [5] any SSEP with $(\lambda, \rho_a, \rho_b)$ can be now mapped to an equilibrium SSEP with $\rho'_a = \rho'_b = \frac{1}{2}$ with corresponding λ' such that

$$\omega(\lambda, \rho_a, \rho_b) = \omega\left(\lambda', \frac{1}{2}, \frac{1}{2}\right) \quad (\text{S-13})$$

By a reparametrization of ρ_a and ρ_b in terms of u and v

$$\rho_a = \frac{e^v \cosh u - 1}{e^v - 1} \quad \text{and} \quad \rho_b = \frac{e^{-v} \cosh u - 1}{e^{-v} - 1} \quad \implies \quad \lambda' = 2u \quad (\text{S-14})$$

the optimal fields can be related by the following transformation $(\rho', \hat{\rho}') \rightarrow (\rho, \hat{\rho})$

$$\rho = \frac{1}{\sinh u \sinh \frac{\lambda}{2}} \left(e^{\hat{\rho}'-u} \sinh \frac{\lambda+u-v}{2} - \sinh \frac{\lambda-u-v}{2} \right) \left(\rho' e^{u-\hat{\rho}'} \sinh \frac{u+v}{2} - (1-\rho') \sinh \frac{u-v}{2} \right) \quad (\text{S-15})$$

$$\hat{\rho} = \log \left[1 + \frac{e^u (e^\lambda - 1) (e^{\hat{\rho}'} - 1)}{e^{\hat{\rho}} (e^u - e^v) + e^u (e^{u+v} - 1)} \right] \quad (\text{S-16})$$

The above transformation keeps the bulk Hamiltonian $H[\rho, \hat{\rho}]$ (S-4), and thus the Euler-Lagrange equations, invariant and also preserves the corresponding structure of the temporal boundary conditions. This can be checked by a direct substitution

$$\hat{\rho}'(x, 1) = \lambda' \implies \hat{\rho} = \lambda \quad \text{with } \lambda' = 2u \quad (\text{S-17})$$

and

$$\hat{\rho}' = \lambda' + \log \frac{\rho'(x, 0)}{1 - \rho'(x, 0)} \implies \hat{\rho} = \lambda + \log \frac{\rho(x, 0)}{1 - \rho(x, 0)} - \log \frac{r(x)}{1 - r(x)} \quad (\text{S-18})$$

The above conditions now lead to

$$\mu(\lambda, \rho_a, \rho_b) = \mu\left(\lambda', \frac{1}{2}, \frac{1}{2}\right) \quad (\text{S-19})$$

with $\omega(\lambda, \rho_a, \rho_b) = \omega(\lambda', \frac{1}{2}, \frac{1}{2})$, we arrive at

$$\mu(\lambda, \rho_a, \rho_b) = \mu\left(2 \operatorname{arcsinh} \sqrt{\omega}, \frac{1}{2}, \frac{1}{2}\right) \quad (\text{S-20})$$

From the above relation, it is evident that $\mu(\lambda, \rho_a, \rho_b)$ depends on λ, ρ_a and ρ_b through a single parameter ω . Since any variational problem with the arbitrary $(\lambda, \rho_a, \rho_b)$ can be mapped similarly, this makes it a general statement for the $\mu(\lambda, \rho_a, \rho_b)$. All these variational problems exhibit equivalence through the invariance of the parameter $\omega(\lambda, \rho_a, \rho_b)$.

$$\text{For our case: } \omega(\lambda, \rho_a, \rho_b) = \omega'(\lambda', \frac{1}{2}, 0) \implies e^\lambda = 2\omega + 1 \quad (\text{S-21})$$

substituting in

$$\mu_{\text{si}}\left(\lambda, \frac{1}{2}, 0\right) = \frac{1}{2\pi} \int_{-\infty}^{\infty} dk \log [1 + (e^{2\lambda} - 1)e^{-k^2}] \quad (\text{S-22})$$

gives the result for arbitrary λ, ρ_a and ρ_b in terms of $\omega(\lambda, \rho_a, \rho_b)$.

NUMERICAL DETAILS: CLONING ALGORITHM

The Cloning Algorithm was first introduced by [7] for discrete time. We follow a continuous-time algorithm to obtain the scgf of Q_T for the semi-infinite lattice which is discussed in [8, 9]. We choose a finite lattice of size L with a reflecting boundary at site L and a reservoir connected at site 0 with the density ρ_a . We initially populate the particles in the bulk with Bernoulli distribution with ρ_b . In Fig. S-1, we have discussed the finite system size, finite time, and finite clone size effects.

INFINITE SSEP WITH MULTIPLE SLOW BONDS: CURRENT FLUCTUATIONS

We consider the SSEP on an infinite one-dimensional lattice. For the sites $i \leq 1$, the hopping rates are taken as α while for sites $i \geq L$, the hopping rates are taken as β (see Fig. S-2). In the between for sites $1 \leq i < L$, the hopping rates are γ . We are looking at the observable Q_T which is the net flux of particles across the finite region i.e., the sites from $i = 0$ to $i = L$. Due to the finite region of size L reaching a quasi-stationary state in time $T \gg L^2$.

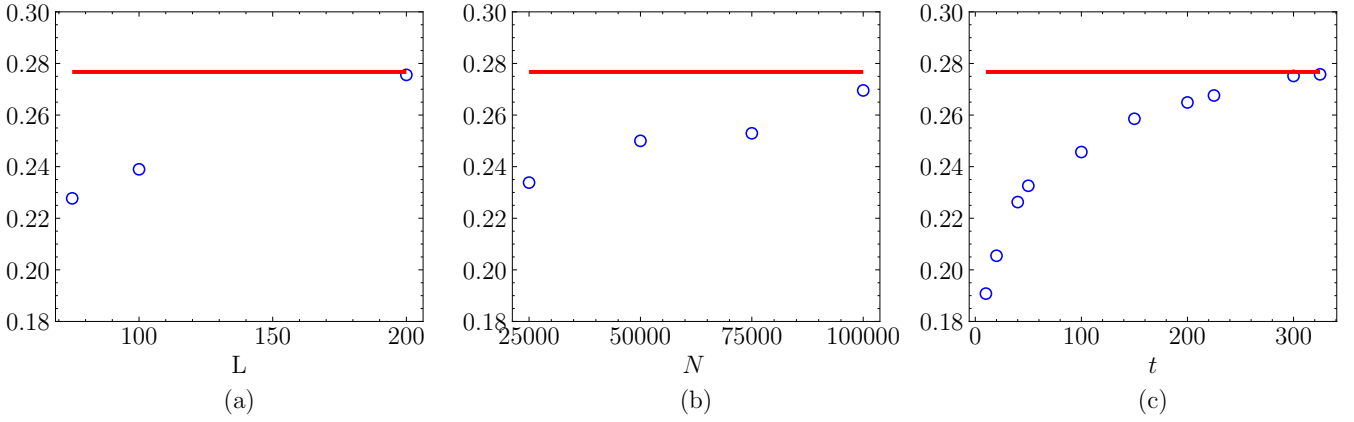


FIG. S-1. We perform numerical verification of the scgf using a cloning algorithm. We couple a reservoir at site $i = 0$ with density ρ_a and implement a reflecting boundary at site $i = L$. We fixed $\rho_a = \rho_b = 0.5$ and $\lambda = 1.0$ for the simulations. In (a), we demonstrate the finite system size effect. We chose $N_c = 5 \times 10^4$, and $t = 250$. It is evident that as the system size increases, the simulation results approach the theoretical results (solid red line) reported in the *Letter*. In (b), we illustrate the finite clone effect. For $t = 250$, and $L = 200$, a large clone size is required to approach the desired exact result. In (c), we present the finite time effect. We chose $L = 200$, and $N_c = 10^5$. Here, it can be observed that a very large time limit is necessary for the numerical results to approach the theoretical results.

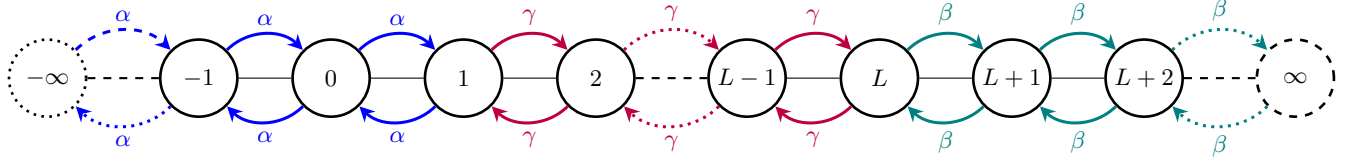


FIG. S-2. Jump rates for different regions of the infinite line

For the left semi-infinite region with $i \leq 0$

$$Y_i(\tau) = \begin{cases} 1 & \text{with prob. } \alpha n_i(\tau) (1 - n_{i+1}(\tau)) d\tau \\ -1 & \text{with prob. } \alpha n_{i+1}(\tau) (1 - n_i(\tau)) d\tau \\ 0 & \text{with prob. } 1 - \alpha [n_i(\tau) (1 - n_{i+1}(\tau)) + n_{i+1}(\tau) (1 - n_i(\tau))] d\tau \end{cases} \quad (\text{S-23a})$$

$$Y_i(\tau) = \begin{cases} 1 & \text{with prob. } \beta n_i(\tau) (1 - n_{i+1}(\tau)) d\tau \\ -1 & \text{with prob. } \beta n_{i+1}(\tau) (1 - n_i(\tau)) d\tau \\ 0 & \text{with prob. } 1 - \beta [n_i(\tau) (1 - n_{i+1}(\tau)) + n_{i+1}(\tau) (1 - n_i(\tau))] d\tau \end{cases} \quad (\text{S-23b})$$

$$Y_i(\tau) = \begin{cases} 1 & \text{with prob. } \gamma n_i(\tau) (1 - n_{i+1}(\tau)) d\tau \\ -1 & \text{with prob. } \gamma n_{i+1}(\tau) (1 - n_i(\tau)) d\tau \\ 0 & \text{with prob. } 1 - \gamma [n_i(\tau) (1 - n_{i+1}(\tau)) + n_{i+1}(\tau) (1 - n_i(\tau))] d\tau \end{cases} \quad (\text{S-23c})$$

while for the right semi-infinite region with $i \geq L$

$$Y_i(\tau) = \begin{cases} 1 & \text{with prob. } \beta n_i(\tau) (1 - n_{i+1}(\tau)) d\tau \\ -1 & \text{with prob. } \beta n_{i+1}(\tau) (1 - n_i(\tau)) d\tau \\ 0 & \text{with prob. } 1 - \beta [n_i(\tau) (1 - n_{i+1}(\tau)) + n_{i+1}(\tau) (1 - n_i(\tau))] d\tau \end{cases} \quad (\text{S-24a})$$

$$Y_i(\tau) = \begin{cases} 1 & \text{with prob. } \alpha n_i(\tau) (1 - n_{i+1}(\tau)) d\tau \\ -1 & \text{with prob. } \alpha n_{i+1}(\tau) (1 - n_i(\tau)) d\tau \\ 0 & \text{with prob. } 1 - \alpha [n_i(\tau) (1 - n_{i+1}(\tau)) + n_{i+1}(\tau) (1 - n_i(\tau))] d\tau \end{cases} \quad (\text{S-24b})$$

$$Y_i(\tau) = \begin{cases} 1 & \text{with prob. } \gamma n_i(\tau) (1 - n_{i+1}(\tau)) d\tau \\ -1 & \text{with prob. } \gamma n_{i+1}(\tau) (1 - n_i(\tau)) d\tau \\ 0 & \text{with prob. } 1 - \gamma [n_i(\tau) (1 - n_{i+1}(\tau)) + n_{i+1}(\tau) (1 - n_i(\tau))] d\tau \end{cases} \quad (\text{S-24c})$$

For the central finite region with $1 \leq i < L$

$$Y_i(\tau) = \begin{cases} 1 & \text{with prob. } \gamma n_i(\tau) (1 - n_{i+1}(\tau)) d\tau \\ -1 & \text{with prob. } \gamma n_{i+1}(\tau) (1 - n_i(\tau)) d\tau \\ 0 & \text{with prob. } 1 - \gamma [n_i(\tau) (1 - n_{i+1}(\tau)) + n_{i+1}(\tau) (1 - n_i(\tau))] d\tau \end{cases} \quad (\text{S-25a})$$

$$Y_i(\tau) = \begin{cases} 1 & \text{with prob. } \alpha n_i(\tau) (1 - n_{i+1}(\tau)) d\tau \\ -1 & \text{with prob. } \alpha n_{i+1}(\tau) (1 - n_i(\tau)) d\tau \\ 0 & \text{with prob. } 1 - \alpha [n_i(\tau) (1 - n_{i+1}(\tau)) + n_{i+1}(\tau) (1 - n_i(\tau))] d\tau \end{cases} \quad (\text{S-25b})$$

$$Y_i(\tau) = \begin{cases} 1 & \text{with prob. } \beta n_i(\tau) (1 - n_{i+1}(\tau)) d\tau \\ -1 & \text{with prob. } \beta n_{i+1}(\tau) (1 - n_i(\tau)) d\tau \\ 0 & \text{with prob. } 1 - \beta [n_i(\tau) (1 - n_{i+1}(\tau)) + n_{i+1}(\tau) (1 - n_i(\tau))] d\tau \end{cases} \quad (\text{S-25c})$$

Given an initial configuration at $\tau = 0$, the system stochastically evolves to reach a given final configuration at $\tau = T \equiv M d\tau$. The generating function of Q_T can then be written as a path integral over all such possible paths of evolution with fixed initial and final configurations as

$$\left\langle e^{\sum_{i=0}^L \Lambda_i Q_i(T)} \right\rangle = \int [Dn] \left\langle \exp \left(\sum_{k=0}^{M-1} \sum_{i=0}^L \Lambda_i Y_i(k d\tau) \right) \left(\prod_{k=0}^{M-1} \prod_{i=-\infty}^{\infty} \delta_{n_i(k d\tau + d\tau) - n_i(k d\tau), Y_{i-1}(k d\tau) - Y_i(k d\tau)} \right) \right\rangle_{[Y]} \quad (\text{S-26})$$

where the path integral measure on the occupation variable is defined as

$$\int [\mathcal{D}n] \equiv \prod_{k=1}^{M-1} \prod_{i=-\infty}^{\infty} \sum_{n_i(k d\tau)=0}^1 \quad (S-27)$$

Using an integral representation of the Kronecker-delta functions and breaking the summation over the lattice site indices for different regions of the infinite line, we get

$$\begin{aligned} \langle e^{\lambda Q_T} \rangle &= \int [\mathcal{D}n] [\mathcal{D}\hat{n}] \exp \left[- \sum_{k=0}^{M-1} \sum_{i=-\infty}^{\infty} \hat{n}_i(k d\tau) (n_i(k d\tau + d\tau) - n_i(k d\tau)) \right] \\ &\quad \left\langle \exp \left[\sum_{k=0}^{M-1} \sum_{i=-\infty}^0 (\hat{n}_{i+1}(k d\tau) - \hat{n}_i(k d\tau) + \Lambda_i \delta_{i,0}) Y_i(k d\tau) \right] \right\rangle_{[Y]} \\ &\quad \left\langle \exp \left[\sum_{k=0}^{M-1} \sum_{i=1}^{L-1} (\hat{n}_{i+1}(k d\tau) - \hat{n}_i(k d\tau) + \Lambda_i) Y_i(k d\tau) \right] \right\rangle_{[Y]} \\ &\quad \left\langle \exp \left[\sum_{k=0}^{M-1} \sum_{i=L}^{\infty} (\hat{n}_{i+1}(k d\tau) - \hat{n}_i(k d\tau) + \Lambda_i \delta_{i,L}) Y_i(k d\tau) \right] \right\rangle_{[Y]} \end{aligned} \quad (S-28)$$

with the path integral measure on the conjugate response variable

$$\int [\mathcal{D}\hat{n}] = \prod_{k=0}^{M-1} \prod_{i=-\infty}^{\infty} \frac{1}{2\pi i} \int_{-\pi}^{\pi} d\hat{n}_i(k d\tau) \quad (S-29)$$

Averaging over the currents for the appropriate regions using (S-23-S-25), the generating function becomes

$$\langle e^{\lambda Q_T} \rangle = \int [\mathcal{D}n] [\mathcal{D}\hat{n}] \exp (\mathcal{K} + \mathcal{H}_{\text{left}} + \mathcal{H}_{\text{centre}} + \mathcal{H}_{\text{right}}) \quad (S-30a)$$

where

$$\mathcal{K} = \sum_{i=-\infty}^{\infty} \left[n_i(0) \hat{n}_i(0) - n_i(T) \hat{n}_i(T) + \int_0^T d\tau n_i(\tau) \frac{d\hat{n}_i(\tau)}{d\tau} \right] \quad (S-30b)$$

$$\mathcal{H}_{\text{left}} = \alpha \sum_{i=-\infty}^0 \int_0^T d\tau \omega (\hat{n}_{i+1}(\tau) - \hat{n}_i(\tau) + \Lambda_i \delta_{i,0}, n_i(\tau), n_{i+1}(\tau)) \quad (S-30c)$$

$$\mathcal{H}_{\text{centre}} = \gamma \sum_{i=1}^{L-1} \int_0^T d\tau \omega (\hat{n}_{i+1}(\tau) - \hat{n}_i(\tau) + \Lambda_i, n_i(\tau), n_{i+1}(\tau)) \quad (S-30d)$$

$$\mathcal{H}_{\text{right}} = \beta \sum_{i=L}^{\infty} \int_0^T d\tau \omega (\hat{n}_{i+1}(\tau) - \hat{n}_i(\tau) + \Lambda_i \delta_{i,L}, n_i(\tau), n_{i+1}(\tau)) \quad (S-30e)$$

with the ω parameter as defined in the *Letter*.

Due to the diffusive nature of the SSEP, we can now assume that the distribution of occupation variables follow a local equilibrium measure defined by a smoothly varying average density field

$$\rho_i(\tau) \simeq \rho \left(\frac{i}{\sqrt{T}}, \frac{\tau}{T} \right) \quad (S-31)$$

where T is the relevant hydrodynamic scale. Furthermore, we assume that the conjugate response variable follows a smoothly varying field

$$\hat{n}_i(\tau) \simeq \hat{\rho} \left(\frac{i}{\sqrt{T}}, \frac{\tau}{T} \right) \quad (S-32)$$

Thus, we can write the leading order behaviour of the generating function for a large T by averaging over the Bernoulli measure

$$n_i(\tau) = \begin{cases} 1 & \text{with prob. } \rho_i(\tau) \\ 0 & \text{with prob. } 1 - \rho_i(\tau) \end{cases} \quad (\text{S-33a})$$

We fix the initial and final configurations such that they can be typically approximated by the initial and final density profiles with $\sum_i n_i(0) \hat{n}_i(0) \simeq \sum_i \rho_i(0) \hat{n}_i(0)$ and $\sum_i n_i(T) \hat{n}_i(0) \simeq \sum_i \rho_i(T) \hat{n}_i(0)$. The generating function then becomes for a large T

$$\langle e^{\lambda Q_T} \rangle \simeq \int [\mathcal{D}n] [\mathcal{D}\hat{n}] \left\langle \exp(\mathcal{K} + \mathcal{H}_{\text{left}} + \mathcal{H}_{\text{centre}} + \mathcal{H}_{\text{right}}) \right\rangle_{[\mathbf{n}]} \quad (\text{S-34})$$

Assuming that for a large T , the probability measures S-33 at different times become independent of one another, we have

$$\langle e^{\lambda Q_T} \rangle \simeq \int [\mathcal{D}\rho] [\mathcal{D}\hat{n}] e^{\sum_{i=-\infty}^{\infty} (\rho_i(0) \hat{n}_i(0) - \rho_i(T) \hat{n}_i(T))} \left(\prod_{\tau} \langle e^{d\tau \mathbb{S}(\tau)} \rangle_{\mathbf{n}(\tau)} \right) \quad (\text{S-35a})$$

with

$$\begin{aligned} \mathbb{S}(\tau) = & \sum_{i=-\infty}^{\infty} n_i(\tau) \frac{d\hat{n}_i(\tau)}{d\tau} + \alpha \sum_{i=-\infty}^0 \omega(\hat{n}_{i+1}(\tau) - \hat{n}_i(\tau) + \Lambda_i \delta_{i,0}, n_i(\tau), n_{i+1}(\tau)) \\ & + \gamma \sum_{i=1}^{L-1} \omega(\hat{n}_{i+1}(\tau) - \hat{n}_i(\tau) + \Lambda_i, n_i(\tau), n_{i+1}(\tau)) \\ & + \beta \sum_{i=L}^{\infty} \omega(\hat{n}_{i+1}(\tau) - \hat{n}_i(\tau) + \Lambda_i \delta_{i,L}, n_i(\tau), n_{i+1}(\tau)) \end{aligned} \quad (\text{S-35b})$$

In the vanishing $d\tau$ limit, we have $\langle \exp(d\tau \mathbb{S}(\tau)) \rangle \simeq 1 + d\tau \langle \mathbb{S}(\tau) \rangle \simeq \exp(d\tau \langle \mathbb{S}(\tau) \rangle)$. Since, the probability measure S-33 is independent for the different lattice sites, the averaging can be readily done by replacing n_i by ρ_i for all i to obtain

$$\langle e^{\lambda Q_T} \rangle \simeq \int [\mathcal{D}\rho] [\mathcal{D}\hat{n}] e^{\mathcal{S}[\rho, \hat{n}]} \quad (\text{S-36a})$$

with

$$\begin{aligned} \mathcal{S}[\rho, \hat{n}] = & \int_0^T d\tau \left\{ - \sum_{i=-\infty}^{\infty} \hat{n}_i(\tau) \frac{d\rho_i(\tau)}{d\tau} + \alpha \sum_{i=-\infty}^0 \omega(\hat{n}_{i+1}(\tau) - \hat{n}_i(\tau) + \Lambda_i \delta_{i,0}, \rho_i(\tau), \rho_{i+1}(\tau)) \right. \\ & + \gamma \sum_{i=1}^{L-1} \omega(\hat{n}_{i+1}(\tau) - \hat{n}_i(\tau) + \Lambda_i, \rho_i(\tau), \rho_{i+1}(\tau)) \\ & \left. + \beta \sum_{i=L}^{\infty} \omega(\hat{n}_{i+1}(\tau) - \hat{n}_i(\tau) + \Lambda_i \delta_{i,L}, \rho_i(\tau), \rho_{i+1}(\tau)) \right\} \end{aligned} \quad (\text{S-36b})$$

where we have used an integration by parts in the τ -variable to simplify the first term.

Finally, taking the diffusively re-scaled space and time $(x, t) \equiv (i/\sqrt{T}, \tau/T)$ and performing a gradient expansion of the fields, we arrive at the leading order behaviour of the generating function for a large T as

$$\langle e^{\lambda Q_T} \rangle \simeq \int [\mathcal{D}\rho] [\mathcal{D}\hat{\rho}] \exp \left[-\sqrt{T} (S_{\lambda_L} + S_{\lambda_C} + S_{\lambda_R}) \right] \quad (\text{S-37a})$$

with

$$S_{\lambda_L}[\rho, \hat{\rho}] = \int_0^1 dt \int_{-\infty}^0 dx \left[\hat{\rho} \partial_t \rho - \alpha \rho (1 - \rho) (\lambda_L \delta(x - 0^-) + \partial_x \hat{\rho})^2 + \alpha \partial_x \rho (\lambda_L \delta(x - 0^-) + \partial_x \hat{\rho}) \right] \quad (\text{S-37b})$$

$$S_{\lambda_C}[\rho, \hat{\rho}] = \int_0^1 dt \int_0^\ell dx \left[\hat{\rho} \partial_t \rho - \gamma \rho (1 - \rho) (\lambda_C + \partial_x \hat{\rho})^2 + \gamma \partial_x \rho (\lambda_C + \partial_x \hat{\rho}) \right] \quad (\text{S-37c})$$

$$S_{\lambda_R}[\rho, \hat{\rho}] = \int_0^1 dt \int_\ell^\infty dx \left[\hat{\rho} \partial_t \rho - \beta \rho (1 - \rho) (\lambda_R \delta(x - \ell^+) + \partial_x \hat{\rho})^2 + \beta \partial_x \rho (\lambda_R \delta(x - \ell^+) + \partial_x \hat{\rho}) \right] \quad (\text{S-37d})$$

where we have suitably scaled the Λ -parameters as $\Lambda_i \simeq (1/\sqrt{T}) \lambda(i/\sqrt{T})$ and denoted $\ell = L/\sqrt{T}$.

Finally, we can now show that (S-37) can be written as

$$\begin{aligned} \langle e^{\lambda Q_T} \rangle &= \int [\mathcal{D}\rho] [\mathcal{D}j] \left[\prod_{t=0}^1 \prod_{x=-\infty}^{\infty} \delta(\partial_t \rho + \partial_x j) \right] \exp \left\{ \int_0^1 dt \left[(\lambda_L j)|_{x=0^-} + \int_0^\ell dx (\lambda_C j) + (\lambda_R j)|_{x=\ell^+} \right] \right\} \\ &\quad \times \exp \left\{ - \int_0^1 dt \left[\int_{-\infty}^0 dx \frac{(j + \alpha \partial_x \rho)^2}{4\alpha\rho(1-\rho)} + \int_0^\ell dx \frac{(j + \gamma \partial_x \rho)^2}{4\gamma\rho(1-\rho)} + \int_\ell^\infty dx \frac{(j + \beta \partial_x \rho)^2}{4\beta\rho(1-\rho)} \right] \right\} \end{aligned} \quad (\text{S-38})$$

which allows us to write the scgf for the infinite line SSEP with a slow region as reported in the *Letter*.

INFINITE SSEP WITH A SINGLE SLOW BOND: FLUCTUATING HYDRODYNAMICS

In this Section, we derive the fluctuating hydrodynamic description for the SSEP on an infinite line with a single slow bond localised at the origin $x = 0$. For this purpose, we set $\alpha = \beta = 1$, $\gamma = \Gamma/\sqrt{T}$ and $L = 2$ as well as $\Lambda_i = 0$. The average hydrodynamic behaviour in similar contexts was studied in [10, 11]. The transition probability to reach a final density profile $\rho(x, t_{\text{fin}})$ starting from an initial density profile $\rho(x, t_{\text{ini}})$ following a stochastic evolution can be obtained following the prescription described in the previous Section [4]. This is given as

$$\Pr[\rho(x, t_{\text{ini}}) \rightarrow \rho(x, t_{\text{fin}})] \simeq \int [\mathcal{D}\rho] [\mathcal{D}\hat{\rho}] \exp \left[-\sqrt{T} \int_{t_{\text{ini}}}^{t_{\text{fin}}} dt (S_{\text{lft}} + S_0 + S_{\text{rgt}}) \right] \quad (\text{S-39a})$$

with

$$S_{\text{lft}}[\rho, \hat{\rho}] = \int_{-\infty}^{0^-} dx \left[\hat{\rho} \partial_t \rho - \rho(1-\rho) (\partial_x \hat{\rho})^2 + \partial_x \rho \partial_x \hat{\rho} \right] \quad (\text{S-39b})$$

$$S_0[\rho, \hat{\rho}] = \Gamma \omega(\hat{\rho}(0^+, t) - \hat{\rho}(0^-, t), \rho(0^-, t), \rho(0^+, t)) \quad (\text{S-39c})$$

$$S_{\text{rgt}}[\rho, \hat{\rho}] = \int_{0^+}^{\infty} dx \left[\hat{\rho} \partial_t \rho - \rho(1-\rho) (\partial_x \hat{\rho})^2 + \partial_x \rho \partial_x \hat{\rho} \right] \quad (\text{S-39d})$$

One can now follow the invert the MSRJD-Action to arrive at the fluctuating hydrodynamics for the bulk regions outside the slow bond

$$\partial_t \rho = \begin{cases} \partial_x^2 \rho + \partial_x \eta_- & \text{for } x < 0 \\ \partial_x^2 \rho + \partial_x \eta_+ & \text{for } x > 0 \end{cases} \quad (\text{S-40a})$$

$$(\text{S-40b})$$

with fluctuating boundaries across the slow bond

$$-\partial_x \rho = \begin{cases} \eta_- + \xi_- & \text{at } x = 0^- \\ \eta_+ + \xi_+ & \text{at } x = 0^+ \end{cases} \quad (\text{S-41a})$$

$$(\text{S-41b})$$

The noises η_- and η_+ are Gaussian with a zero mean and their covariances are delta-correlated in space and time such that

$$\langle \eta_-(x, t) \eta_-(x', t') \rangle = \frac{1}{\sqrt{T}} [2\rho(1-\rho)] \delta(x-x') \delta(t-t') \theta(-x) \quad (\text{S-42})$$

$$\langle \eta_+(x, t) \eta_+(x', t') \rangle = \frac{1}{\sqrt{T}} [2\rho(1-\rho)] \delta(x-x') \delta(t-t') \theta(x) \quad (\text{S-43})$$

with $\langle \eta_-(x, t) \eta_+(x', t') \rangle = 0$. The noises ξ_- and ξ_+ are Poissonian which are delta-correlated in time with their joint moment-generating function given by

$$\left\langle \exp \left[\int dt (\hat{\rho}(0^+, t) \xi_+(t) - \hat{\rho}(0^-, t) \xi_-(t)) \right] \right\rangle_{\xi_+, \xi_-} \simeq \exp \left[\Gamma \int dt \omega(\hat{\rho}(0^+, t) - \hat{\rho}(0^-, t), \rho(0^-, t), \rho(0^+, t)) \right] \quad (\text{S-44})$$

RECOVERING THE INFINITE LINE RESULTS

We take the results of the scgf as presented in the *Letter*

$$\mu_{\text{inf}}^{(\text{slow})}(\lambda, \rho_a, \rho_b) = \min_{z_a, z_b} \left[R_{\text{si}}(\sinh^2 z_a) + \frac{\Gamma}{L} (z_a + z_b - u)^2 + R_{\text{si}}(\sinh^2 z_b) \right] \quad (\text{S-45})$$

with $u = \text{asrcsinh} \sqrt{\omega(\lambda, \rho_a, \rho_b)}$ and look at the limit of $\Gamma \rightarrow \infty$. This corresponds to the case when the central region becomes equally fast as compared to the regions outside. In that case, the second term dominates and we find that the minimisation over z_a and z_b leads to the solutions $z_a = z_b = u/2$. Putting this in the above expression, we find

$$\mu_{\text{inf}}^{(\text{fast})}(\lambda, \rho_a, \rho_b) = 2 R_{\text{si}}\left(\sinh^2 \frac{u}{2}\right) = 2 R_{\text{si}}(\omega(\lambda, \rho_a, \rho_b)) \quad (\text{S-46})$$

Using the expression of the scgf $\mu_{\text{si}}(\lambda, \rho_a, \rho_b) = R_{\text{si}}(\omega(\lambda, \rho_a, \rho_b))$ as in the *Letter*, we can further simplify the above expression to obtain

$$\mu_{\text{inf}}^{(\text{fast})}(\lambda, \rho_a, \rho_b) = \int_{-\infty}^{\infty} \frac{dk}{\pi} \log [1 + \omega(\lambda, \rho_a, \rho_b) e^{-k^2}] \quad (\text{S-47})$$

which is the seminal result for the infinite line SSEP as reported in [12, 13]. This demonstrates one self-consistency check for the exact semi-infinite result as well as the variational result for the infinite line with a finite slow region.

* kapil.sharma@tifr.res.in

† soumyabrata.saha@tifr.res.in

‡ sandeep.jangid@tifr.res.in

§ tridib@theory.tifr.res.in

- [1] S. Saha and T. Sadhu, Current fluctuations in a semi-infinite line, *J. Stat. Mech.* **2023**, 073207 (2023).
- [2] C. Erignoux, P. Gonçalves, and G. Nahum, Hydrodynamics for SSEP with non-reversible slow boundary dynamics: Part I, the critical regime and beyond, *J. Stat. Phys.* **181**, 1433–1469 (2020).
- [3] C. Erignoux, P. Gonçalves, and G. Nahum, Hydrodynamics for SSEP with non-reversible slow boundary dynamics: Part II, below the critical regime, *ALEA, Lat. Am. J. Probab. Math. Stat.* **17**, 791–823 (2020).
- [4] S. Saha and T. Sadhu, Large deviations in the symmetric simple exclusion process with slow boundaries: A hydrodynamic perspective (2023), [arXiv:2310.11350v2 \[cond-mat.stat-mech\]](https://arxiv.org/abs/2310.11350v2).
- [5] B. Derrida and A. Gerschenfeld, Current fluctuations in one dimensional diffusive systems with a step initial density profile, *J. Stat. Phys.* **137**, 978–1000 (2009).
- [6] V. Lecomte, A. Imparato, and F. van Wijland, Current fluctuations in systems with diffusive dynamics, in and out of equilibrium, *Prog. Theor. Phys. Suppl.* **184**, 276–289 (2010).
- [7] C. Giardina, J. Kurchan, and L. Peliti, Direct evaluation of large-deviation functions, *Phys. Rev. Lett.* **96**, 120603 (2006).
- [8] V. Lecomte and J. Tailleur, A numerical approach to large deviations in continuous time, *J. Stat. Mech.* **2007**, P03004 (2007).
- [9] C. Pérez-Espigares and P. I. Hurtado, Sampling rare events across dynamical phase transitions, *Chaos* **29**, 083106 (2019).
- [10] T. Franco, P. Gonçalves, and A. Neumann, Hydrodynamical behavior of symmetric exclusion with slow bonds, *Ann. Inst. H. Poincaré Probab. Statist.* **49**, 402–427 (2013).
- [11] D. Erhard, T. Franco, P. Gonçalves, A. Neumann, and M. Tavares, Non-equilibrium fluctuations for the SSEP with a slow bond, *Ann. Inst. H. Poincaré Probab. Statist.* **56**, 1099–1128 (2020).
- [12] B. Derrida and A. Gerschenfeld, Current fluctuations of the one dimensional symmetric simple exclusion process with step initial condition, *J. Stat. Phys.* **136**, 1–15 (2009).
- [13] K. Mallick, H. Moriya, and T. Sasamoto, Exact solution of the macroscopic fluctuation theory for the symmetric exclusion process, *Phys. Rev. Lett.* **129**, 040601 (2022).

